JCTC Journal of Chemical Theory and Computation

Metal−Molecule Interactions To Produce Hydrogen: What Do They Have in Common?†

Job Valdespino-Saenz, Alfredo Guevara-García, Marco-Vinicio Vázquez, and Ana Martínez*

Instituto de Investigaciones en Materiales, Universidad Nacional Autónoma de México, Circuito Exterior s/n, C. U., P.O. Box 70-360, Coyoacán 04510, México, D. F. México

Received December 13, 2006

Abstract: The main purpose of this work is to study metal−molecule interactions that can lead to the production of molecular hydrogen. Two systems were chosen for this analysis: yttrium atom and clusters interacting with the simple electron donor ammonia (NH_3) and copper atoms and ions with imidazole. For yttrium with ammonia as well as for copper with imidazole there is a charge-transfer process from the metal to the molecule that promotes the dissociation of the hydrogen atoms.

Introduction

Human population growth has severe consequences for the environment. One negative factor is pollution caused by the emission of several gases related to the widespread use of carbon-containing fuels. The emission of greenhouse gases into the atmosphere is increasing due to a constantly growing world energy demand and the amount of fossil fuels being burned in order to meet that demand. The development of zero emission energy production systems is one of the major goals of many research efforts. The most attractive option with regards to sustainability is the use of molecular hydrogen as a fuel.[1]

It is well-known that in order to be sustainable, the hydrogen production process must be water based, with no consumption of raw materials and with zero emissions of greenhouse gases. Electrolysis at low temperature is one of the options, but, for the time being, that is more expensive than the production of hydrogen from natural gas. Making hydrogen using steam has two disadvantages, namely, that the process consumes natural gas, another carbon-based nonrenewable source, and produces carbon dioxide. Recently, the manufacture of hydrogen by electrolysis at high temperature[2] has been reported. It is a promising idea that could be used in the Icelandic geothermal context; however, the appropriate heat exchangers necessary for this process are still under development.

Nevertheless, the production of hydrogen from water is not the only available option. There are many chemical interactions that have hydrogen as one of the main products of the reaction. Heterogeneous catalysis is one of several procedures that can be used for this end. For the further development of heterogeneous catalysis, the analysis of the nature of the interaction between small molecules or radicals and transition metals is very important. For this reason, the reactivity of transition metals with numerous molecules and radicals has been the subject of several studies.[3−17] Many of these studies focused on the reaction of transition-metal atoms and clusters, and it was considered that the understanding of their reactivity with small molecules could shed light upon several mechanisms of surface chemistry and provide details of complicated processes associated with heterogeneous catalysis. By considering only the processes that produce hydrogen, we could arrive at the knowledge necessary for the development of a water independent hydrogen fuel technology.

Concerning the interactions of transition-metal atoms and clusters with molecules that produce hydrogen, there have been several studies reported recently. For example, some groups have studied the dehydrogenation reactions of organic molecules with Nb clusters and cluster cations.[18−21] In particular, ethene chemistry is well characterized for neutral transition-metal atoms reactions in the gas phase. These reactions with niobium atoms and clusters indicate dehydrogenation of ethene for all clusters, the extent of the

† Dedicated to Dennis R. Salahub on the occasion of his 60th birthday.

* Corresponding author phone: (5255) 56 22 45 96; fax: (5255) 56 16 12 51; e-mail: martina@iim.unam.mx.

10.1021/ct6003615 CCC: $37.00
Published on Web 02/24/2007

reactivity depending on cluster size.[21] The reactions of Nb clusters with ethane lead to partially or fully dehydrogenated products, involving mechanistic steps that are generally barrierless. On the other hand, the dehydrogenation reaction by a bare Nb atom and a cation[22] proceeds by the formation of a molecular hydrogen complex that releases hydrogen without an energy barrier.

Other studies consider different aspects, but they are also related to the formation of molecular hydrogen. For example, DNA bases and their interaction with metal atoms have been studied in order to analyze structural information that could be relevant to the knowledge of metal effects on biological processes.[23] Despite the fact that the subject of these studies is not the production of hydrogen, the results show that for guanine−Cu and uracil−Cu anionic, it is possible to produce the detachment of one electron from the anion and also the removal of one hydrogen atom, with the consequent formation of molecular hydrogen. This could happen because the vertical ionization energy of the anion is close to the dissociation energy of one hydrogen atom. Elsewhere, oxidative additions at the metal centers have been studied due to their importance in organometallic reactions in homogeneous catalysis.[24] The first observation of the yttrium imide (YNH) molecule in gas phase was made with laser vaporization of yttrium metal in a molecular beam, using an He/NH_3 mixture as a carrier gas.[25] In that study, the interaction of yttrium atoms with ammonia was examined, and it was reported that the reaction proceeds by the formation of a $M-NH_3$ molecular complex followed by an oxidative addition. The formation of an yttrium imide molecule (YNH) in the gas phase could also produce molecular hydrogen.

Within this framework, the main purpose of this work is to study metal−molecule interactions that can lead to the production of molecular hydrogen. Two systems were chosen for this analysis: yttrium atom and clusters interacting with the simple electron donor ammonia (NH_3) and copper atoms and ions with imidazole. The noncovalent interaction with metal ions present in the latter system is a simple model for a wide variety of nitrogen-containing heterocycles. Both systems contain a transition-metal atom with one unpaired electron. The idea is to find the relationship between the electronic structure and the reactivity of these systems, in search of the production of hydrogen molecules. With this objective, optimized geometries, net atomic charges, and molecular orbitals are reported for $Y-NH_3$, Y_2-NH_3, and $Cu-(imidazole)_N$ ($N = 1-3$, neutral and anionic), and several reaction mechanisms are also analyzed.

Aromaticities computed via the HOMA indexes for the imidazole molecules are reported, in order to analyze the aromatic character of these systems. HOMA index can be used to estimate an aromatic character of π-electron systems (molecules, ions, or their fragments).

Computational Details

Density functional theory,[26−28] as implemented in the suite of programs *Gaussian 03*,[29] has been used to carry out all calculations. The hybrid three parameters B3LYP[30−32] functional and the LANL2DZ[33−45] basis set were used to perform complete optimizations of molecular geometries without symmetry constraints. Harmonic frequencies analyses[36,37] allowed us to verify optimized minima.

Previous studies show that DFT reproduces equilibrium geometries and relative stabilities with hybrid functionals, which partially include the Hartree−Fock exchange energy. The results are in good agreement with those obtained using the Møller−Plesset perturbational theory at second order and basis sets of medium quality, such as 6-31G(d,p), and cc-pVDZ.[38−40] For this reason, in this work, we are confident of the results obtained with B3LYP.

The number of isomers used in the initial stage of the study provided several initial geometries, which, in turn, allowed us to widely explore the potential energy surface, in search of the global minimum. Notwithstanding the difficulties associated with the localization of the ground states, we cannot exclude the possibility that the global minimum could be missed. Nonetheless, the number of initial geometries examined was large enough to reliably identify the global minima in each system.

To compute vertical electron detachment energies (VEDE) of anionic species and vertical ionization potentials of the neutrals, further single-point calculations were required. Formation energies for neutral and anionic species were calculated using zero-point corrected energies.

Although there is no universally accepted method of assigning electrostatic charges to atoms, and no experimental technique is actually available to measure them directly, in a former study, de Oliveira et al.[41] reported the testing of the quality of charges obtained via the Mulliken and Bader population analysis methods. Those authors found a good agreement between the methods, taking into account the qualitative description of the atomic charges. Thus, in this paper, Mulliken atomic charges are used to discuss the qualitative behavior of the charge-transfer process.

The HOMA (harmonic oscillator model of aromaticity) method[42] was used as reported by Krygowski.[43−46] The bond lengths of the optimized structures were employed for the study of aromaticity with this model.

Visualization of the results was carried out using the Molekel[47−49] and the Ball&Stick[50] packages.

Results and Discussion

Y and Y_2 with Ammonia. Our study is primarily stimulated by experimental results, obtained some time ago,[51] concerning the reactivity of the yttrium atom toward ammonia, at room temperature, in a fast-flow reactor. The yttrium nitride species from these experiments were detected in ionization but created as neutral. The results gave as very prominent species Y_2N, Y_3N_2, Y_4N_3, Y_5N_4, Y_6N_5, Y_7N_6, and Y_8N_7. Nevertheless, the authors of a previous study reported[52] that the first step of the reaction is the formation of yttrium imide (YNH) through the oxidative addition of the N−H bond of ammonia and the elimination of molecular hydrogen. With this in mind, in this study, we analyze the interaction of ammonia with yttrium atom and dimer. In Table 1, we report the systems considered in this paper. The selection of these molecules is related to the available experimental informa-

Table 1. Vertical and Adiabatic Ionization Potentials (in eV) of the Systems Considered in This Work for the Interaction of Yttrium with Ammonia[a]

	2S+1	calcd vertical IP (eV)	calcd adiabatic IP (eV)	exptl IP (eV)
Y_2	5	5.07	5.04	4.98
YNH	2	5.95	5.94	5.84
YN	1	6.38	6.37	~6.4
A Y_2NH	1	5.41	5.20	5.5
B Y_2NH	1	5.64	5.21	5.5
C Y_2NH	3	5.16	5.11	5.5
$Y_2N\ ^2B_2$	2	5.30	5.20	4.4
$Y_2N\ ^2B_1$	2	4.58	4.46	4.4
Y_3N_2H	3	4.74		
Y_3N_2	2	4.54	4.50	4.27

[a] Experimental available information is also shown (Simard, private communication).

tion, since we used the ionization potentials to validate the results. In Table 1, vertical and adiabatic ionization potentials for the most stable structures are reported. Available experimental results are also shown. Experimentally, ionization potentials are always vertical. It may happen that they correspond to adiabatic when there is a major change in structures, but this is not the case for these systems. As may be observed, theoretical values are in good agreement with experimental results, except for Y_2N ($^2B_2$ electronic state). The reason for this disagreement between experimental and calculated ionization potentials can be that the excitation arise from high lying vibrational states or low lying electronic states. The observed ionization potential value is smaller than the calculated one. This is possible because the Y_2N may be excited by the plasma originating from the laser vaporization source.[51] The calculated vertical IP value for an excited state (17.1 kcal/mol less stable, $^2B_1$ electronic state) matches quite well with the experimental value (see Table 1). However, for further discussion we will use $^2B_2$ electronic state, given that it is more stable. Comparing experimental values with theoretical values in Table 1, it is readily apparent that, in most cases, the calculated ionization potential is overestimated. The only theoretical value that is underestimated with respect to the experiment is that for Y_2NH. For this system, other structures were considered for the optimization. In Figure 1, Y_2NH optimized structures are reported. In Table 1, the corresponding IP theoretical values are also reported. As may be observed, the promotion of an hydrogen atom toward the metal atom leads us to a more stable structure (by 4.1 kcal/mol). The ground state is a specie that contains one hydrogen atom interacting with two metal atoms. The hydrogen atomic charge is positive in the Y_2NH (imide), while it is negative for the other structures. The energy difference between these species is very small, and we may consider that we are at the limits of the calculation. Comparing the experimental IP with the theoretical values reported in Table 1 for these isomers, it is apparent that agreement is more or less the same for the three structures. With these results, it is not possible to say that one structure is more stable than the others. Further studies, now in progress, consider the energy barriers and possible transition states necessary to determine whether the hydrogen atom is

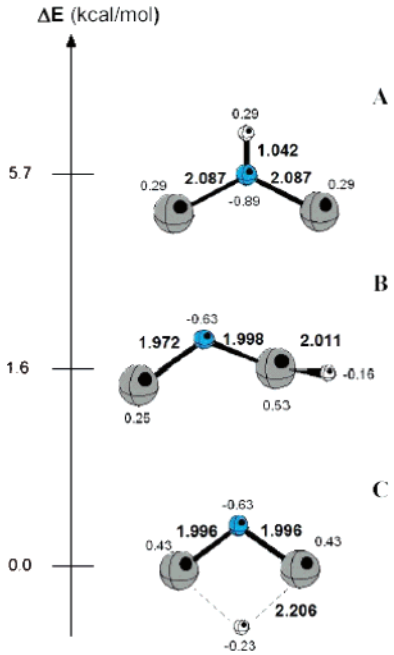

Figure 1. Relative stability between optimized Y_2NH isomers.

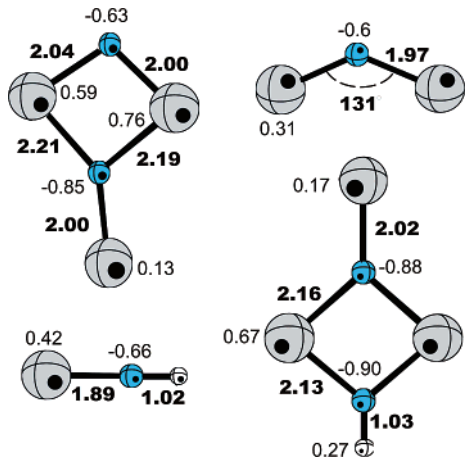

Figure 2. Optimized geometries for the most stable isomers of the Y_mN_x and Y_mN_xH species. Bond lengths, in Å, and atomic charges, in au, are also shown.

bound to the metal or not. At this point, and for this study, the discussion will continue with Y_2NH (imide), since we would like to compare the results with those obtained for YNH and Y_3N_2H.

Optimized structures of the systems considered in this work are reported in Figures 1 and 2. All species are neutral. The first reaction of ammonia with the yttrium atom has been described as an oxidative addition to produce yttrium imide (YNH).[17,25] The reported Y−N bond distance is 1.877 Å and 1.926 Å, for experimental and theoretical values, respectively.[17] As can be seen in Figure 1, the optimized bond length (1.89 Å) is in very good agreement with the experimental value. In addition, the error in the calculated ionization energy is minor, and it is possible to say that the difference is small enough for a reliable assignment of YNH stable structure.

In Figures 1 and 2, Y_2N and Y_2NH are observed to have a bent structure, with a bond angle close to 130 degrees.

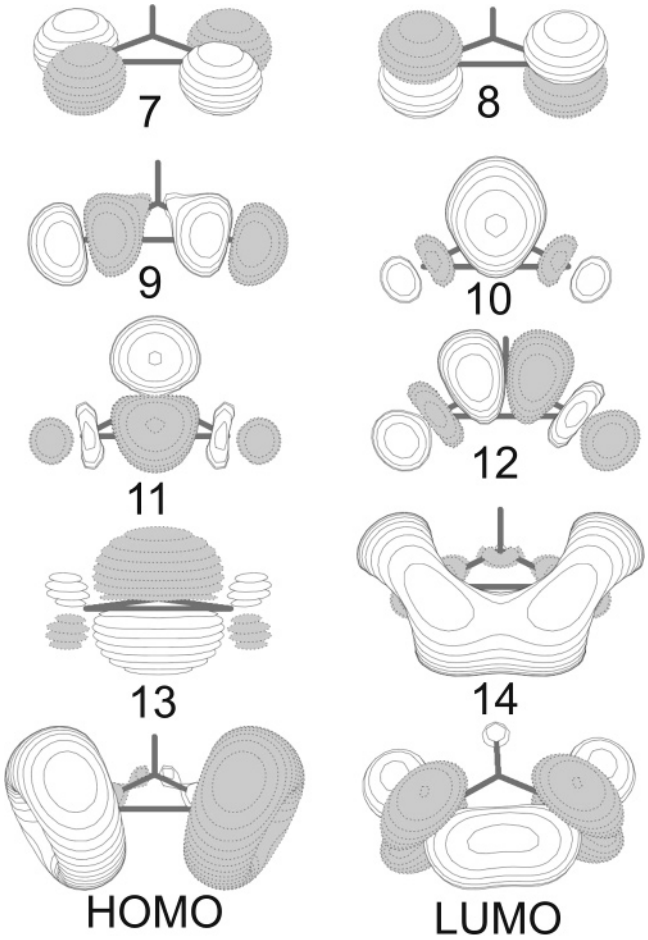

Figure 3. Molecular orbital pictures of Y_2NH.

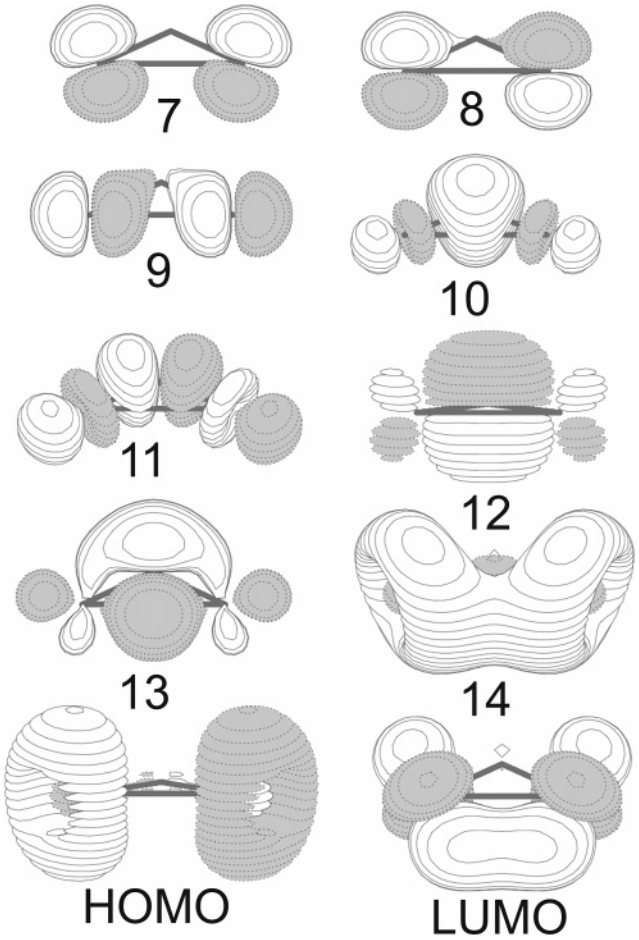

Figure 4. Molecular orbital pictures of Y_2N.

Y−N bond length is shorter for Y_2N than for Y_2NH (imide). Molecular orbital pictures reported in Figures 3 and 4 (for Y_2NH and Y_2N, respectively) are quite similar. The exception is orbital 11. For Y_2NH, this orbital has an antibonding interaction between N and the metal atoms, and this explains the differences in the bond distances with respect to Y_2N. The bent structure is promoted by the bonding interaction of the yttrium d orbitals in both systems. HOMO are nonbonding orbitals located on the metal atoms, while the LUMO is a metal−metal antibonding orbital. As Figure 2 shows, this bent shape is observed in all of the systems. Moreover, with and without the hydrogen atom, the structures for Y_3N_2 and Y_3N_2H are very similar.

For all species, the analysis of the net atomic charges from the Mulliken population analyses indicates that metal atomic charges are positive, while nitrogen atomic charges are negative, as might be expected. There is a charge-transfer process from the Y atoms to either the NH moiety or the N atom. At the beginning of the reaction, it may be considered that there is a donation of the electron pairs from the ammonia molecule to the metal atoms. For this donation, the vacant orbitals of the yttrium atoms play a fundamental role. After this dative bond is formed, there is a back-donation to the p orbitals of N. The charge-transfer process from the Y atoms to the NH moiety promotes the dissociation of the ammonia molecule. It appears that the reaction mechanism involves a charge-transfer process from the Y to the ammonia.

Table 2. Formation Energies (in kcal/mol) for the Reactions Schemes under Study, for the Interaction of Yttrium with Ammonia

	reaction	ΔE (kcal/mol)
A	**2** YNH → **2** YN + H_2	107.4
B	Y + YNH → Y_2NH	−65.0
C	Y + YNH → Y_2N + H	−10.7
D	Y_2NH + YNH → Y_3N_2 + H_2	−69.8
E	Y_2N + YNH → Y_3N_2H	−90.8
F	Y_2N + YNH → Y_3N_2 + H	−19.7
G	Y + Y → Y_2	−25.5
H	Y + NH_3 → YNH + H_2	−30.6
I	Y_2 + NH_3 → Y_2NH + H_2	−70.2

In order to analyze the reaction for the production of molecular hydrogen, Table 2 reports the binding energies for different reaction paths. For these analyses, only the molecules with experimental determination of the ionization potential were considered. The exception is Y_3N_2H, since the experimental value has not yet been determined, and we use the optimized structure as the product of one of the reactions.

The YNH molecule may perhaps interact with different reactants that could be present in the experiment. The first consideration for the reaction of yttrium imide is the

interaction between two equal molecules (scheme A in Table 2). The reaction produces YN and H_2. As may be observed, this reaction is not energetically feasible, given that the products of the reaction are less stable than the reactants by more than 100 kcal/mol. Yttrium imide could also interact with yttrium atoms, yielding Y_2NH or Y_2N and atomic hydrogen (schemes B and C, Table 2). In both cases, the products are more stable than the reactants. Comparing these two reactions, it is energetically more favorable to produce Y_2NH than Y_2N plus H.

After the formation of YNH, Y_2NH, and Y_2N, these three molecules could join up in such a way that they produce a cluster with three yttrium atoms, nitrogen, and with or without hydrogen, as may be observed in Table 2 (schemes D−F). Y_2NH and YNH react to form Y_3N_2 plus molecular hydrogen (path D). The stabilization energy is close to 70 kcal/mol, so the formation of molecular hydrogen seems to be energetically feasible. On the other hand, YNH interacts with Y_2N, and there are two possible paths for the reaction: the formation of Y_3N_2H (scheme E) or the production of Y_3N_2 and H (scheme F). The experimental ionization potential for Y_3N_2H has not been reported as yet, so we do not know if it is possible to obtain this product in the experiment. Comparing both reactions, we may say that it is energetically more stable to produce Y_3N_2H than Y_3N_2 and H.

It is not only the Y atom that is capable of reacting with ammonia to form H_2, given that Y_2 is also a potential reactant. We may suppose, however, that Y and ammonia are at the beginning of the reaction. The first interaction produces YNH and H_2 and also Y_2. Looking at the values in Table 2, it may be observed that the binding energies are similar for both reactions (−30.6 and −25.5 kcal/mol, for the formation of YNH and Y_2, respectively). After this first interaction, ammonia, Y, Y_2, and YNH could be present in the reactor. The dimer can interact with ammonia to form Y_2NH and H_2; yttrium could react with YNH to form Y_2NH (schemes I and B, respectively), and, once again, the binding energies for these two processes are comparable. In Figure 5, the scheme of the reaction between Y_2 and ammonia is reported. As may be observed, there is a first approximation of the ammonia molecule to one of the metal atoms, followed by the formation of Y_2NH and H_2. The energy differences indicate that both interactions are feasible, since the products are more stable than the reactants. The most probable reaction is the formation of Y_2NH and H_2, because H_2 is a relatively stable molecule. Comparing this reaction with the formation of Y_2NH, starting from Y and YNH (path B), it is possible to say that the stability is fairly similar. If Y, Y_2, and YNH are together in the experiment with ammonia, it is probable that Y_2NH will be formed, with the consequent production of H_2.

From all these reactions, it is possible to conclude that YNH could react with Y_2NH to produce H_2 and that the yttrium dimer is a possible reactant also, producing molecular hydrogen and Y_2NH. These results consider that ammonia is the limiting reactant. If ammonia is in excess, we should consider other interactions with ammonia as we did in a previous study.[52] In that prior report, experimentally and

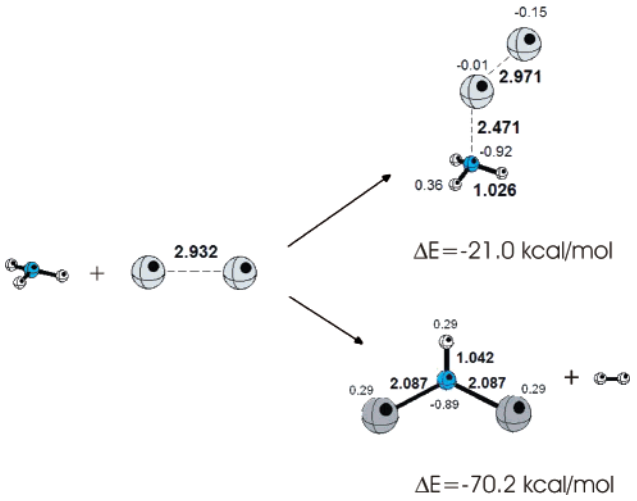

Figure 5. Reaction between NH_3 and Y_2. Two possible paths, one with NH_3 simply adsorbed to Y_2, and the other with H_2 production. Bond lengths are in Å, and atomic charges in au are also shown.

theoretically, we concluded that yttrium imide reacts with ammonia to form a species with the general formula $YNH(NH_3)_n$. DFT calculations revealed evidence supporting the dissociative absorption of NH_3 by YNH to form $Y(NH_2)_2$. This diamide specie can absorb additional NH_3 molecules to form $Y(NH_2)_2NH_3$, $Y(NH_2)_2(NH_3)_2$, and $Y(NH_2)_2(NH_3)_3$. The diamide species are more stable than the imide complexes ($YNH(NH_3)_n$) by approximately 30 kcal/mol. These stabilization energies are similar to the energy differences reported in Table 2 for the interactions between Y atoms to form Y_2; however, the formation of the diamide species is energetically less favorable than the formation of Y_2NH (from Y_2 plus NH_3), Y_3N_2 (from Y_2NH plus YNH), and Y_3N_2H (from Y_2N and YNH) (see Table 2). In accordance with that stated up to this point, oxidative addition is the first step of the reaction of the yttrium atom with ammonia to form the imide species. Yttrium atoms could also interact and yttrium dimers will be formed, since the binding energies are similar (−30.6 and −25.5 kcal/mol). If ammonia is the limiting reactant, it is most probable that YNH will react with Y, Y_2NH, and Y_2N, as may be observed in Table 2. If Y_2 is already formed, then the addition of one ammonia molecule to Y_2 to form $Y_2NH + H_2$ will occur. If the dimer is not formed because ammonia is in excess and the most probable reaction is the formation of YNH, then we may consider that the sequential addition of three further NH_3 molecules to YNH, in order to produce the diamide species, is a possible reaction. Nonetheless, the formation of the diamide species is energetically less favorable, so it is possible to say that, in the presence of YNH, Y, Y_2, and ammonia, the most energetically favorable reactions include the formation of Y_2NH and H_2.

Currently, the optimum reactions for the production of H_2 are with Y_2NH and YNH (path D in Table 2) and Y_2 with ammonia (path I). YNH could also react with ammonia molecules to form the diamide species. To avoid competition with the diamide formation, it is preferable to have ammonia as the limiting reactant. If this is the case, it is possible to control the experiment in order to have only the following

Table 3. Anionic and Neutral $C_3H_4N_2Cu$ Optimized Geometries[a]

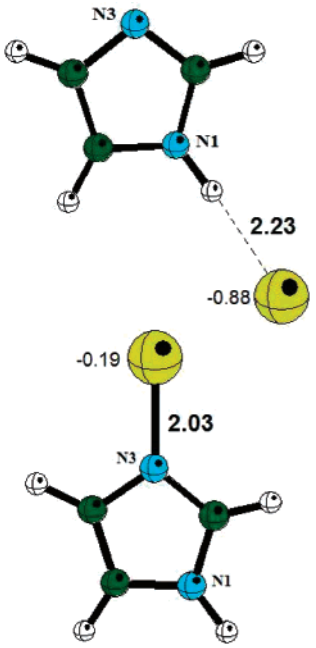

Anion

Bond lengths		Atomic charges	
N1-C2	1.38	N1	-0.29
C2-N3	1.35	C2	-0.21
N3-C4	1.40	N3	-0.15
C4-C5	1.40	C4	-0.32
C5-N1	1.39	C5	-0.21

HOMA: 0.82

Neutral

Bond lengths		Atomic charges	
N1-C2	1.38	N1	-0.33
C2-N3	1.34	C2	-0.07
N3-C4	1.40	N3	-0.21
C4-C5	1.38	C4	-0.15
C5-N1	1.40	C5	-0.20

HOMA: 0.79

[a] Bond lengths are in Å, atomic charges in au.

reactions that are energetically viable:

$$Y + NH_3 \rightarrow YNH + H_2$$

$$YNH + Y \rightarrow Y_2NH$$

$$Y_2NH + YNH \rightarrow Y_3N_2 + H_2$$

If the production of Y_2 is controlled, then it is possible to obtain molecular hydrogen through the following reaction:

$$Y_2 + NH_3 \rightarrow Y_2NH + H_2$$

The nature of the relationship between the size of the metal cluster and the reactivity of these clusters with ammonia is still an open question, and further calculations are in progress in an attempt to find an answer.

Cu−(imidazole)$_N$ (N = 1−3). Imidazole has a five-membered planar ring structure. Two p electrons are located on N1; N3 and the three carbon atoms provide one p electron each to form a sextet aromatic π system. Additionally, N3 has a lone pair of electrons in the plane of the molecule. Consequently, imidazole has multiple binding sites and could interact with atoms or molecules as an aromatic π ligand or as a simple σ ligand.[53] In this study, the interaction of imidazole molecules with copper atoms is analyzed (neutral and anionic). The study of the anionic species is important because we would like to know if it is possible to obtain molecular hydrogen from these compounds. Given that there is an electronic repulsion between the copper atom and the imidazole molecule in the Cu−imidazole (neutral) system, we may consider that this electronic repulsion will be bigger in the anionic species. Other studies on anions, such as Cu−guanine and Cu−uracil,[23] conjectured that it could be possible to produce the dissociation of one hydrogen atom

Table 4. Anionic and Neutral $C_3H_3N_2Cu$ Optimized Geometries[a]

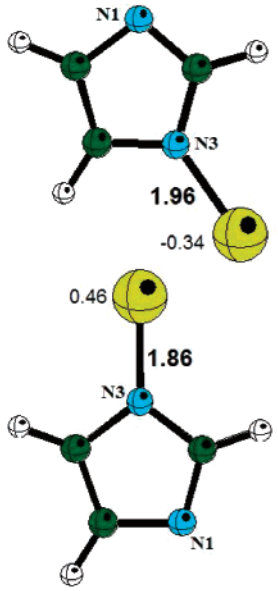

Anion

Bond lengths		Atomic charges	
N1-C2	1.36	N1	-0.17
C2-N3	1.38	C2	-0.23
N3-C4	1.40	N3	-0.29
C4-C5	1.40	C4	-0.23
C5-N1	1.40	C5	-0.37

HOMA: 0.80

Neutral

Bond lengths		Atomic charges	
N1-C2	1.34	N1	-0.12
C2-N3	1.39	C2	-0.17
N3-C4	1.41	N3	-0.39
C4-C5	1.39	C4	-0.17
C5-N1	1.40	C5	-0.31

HOMA: 0.75

[a] Bond lengths are in Å, atomic charges in au.

Table 5. Reactions of Cu−(imidazole)$_N$ Species with H_2 Production[a]

	reaction	ΔE (kcal/mol)
I	**2** $C_3H_4N_2Cu \rightarrow$ **2** $C_3H_3N_2Cu + H_2$	9.3
II	**2**$(C_3H_4N_2Cu)^{-1} \rightarrow$ **2**$(C_3H_3N_2Cu)^{-1} + H_2$	−12.8
III	$(C_3H_4N_2)_2Cu \rightarrow (C_3H_3N_2)_2Cu + H_2$	7.0
IV	$[(C_3H_4N_2)_2Cu]^{-1} \rightarrow [(C_3H_3N_2)_2Cu]^{-1} + H_2$	−48.9
V	$(C_3H_4N_2)_3Cu \rightarrow (C_3H_4N_2)_2Cu(C_3H_2N_2) + H_2$	14.5
VI	$[(C_3H_4N_2)_3Cu]^{-1} \rightarrow [(C_3H_4N_2)_2Cu(C_3H_2N_2)\,]^{-1} + H_2$	−32.9

[a] Reaction energies are in kcal/mol.

from these species. According to this thesis, it is necessary that we study the neutral and anionic Cu−(imidazole)$_N$ compounds, in order to ascertain whether the dissociation of hydrogen is energetically favorable.

Table 3 reports the optimized structure of Cu−imidazole (neutral and anionic). Bond lengths and atomic charges are also shown. In a previous work, Wang et al.[54] reported an experimental and theoretical study of Al and Cu−imidazole, neutral and cationic. They produced Al and Cu−imidazole in laser-vaporization supersonic molecular beams, determined the zero electron kinetic energy (ZEKE) spectrum, and used the second-order Moller−Plesset (MP2) theory to perform a theoretical study. The σ structure was found to be more stable than the π structure. The weakness of this bond between Cu and imidazole is attributed to the antibonding (HOMO) interaction and the electron repulsion between the N lone-pairs and the Cu 4s electrons. Comparing the optimized structures for Cu−imidazole at the MP2 level with the structure that we obtained with B3LYP and LANL2DZ (see Table 3), it may be said that they are in good agreement. The optimized Cu−N bond distance is 1.978 and 2.03 Å, for MP2 and B3LYP, in that order. The electronic state is the same ($^2A'$). This comparison is useful for validating our

Table 6. Anionic (**A**) and Neutral (**B**) $(C_3H_4N_2)_2Cu$ Optimized Geometries[a]

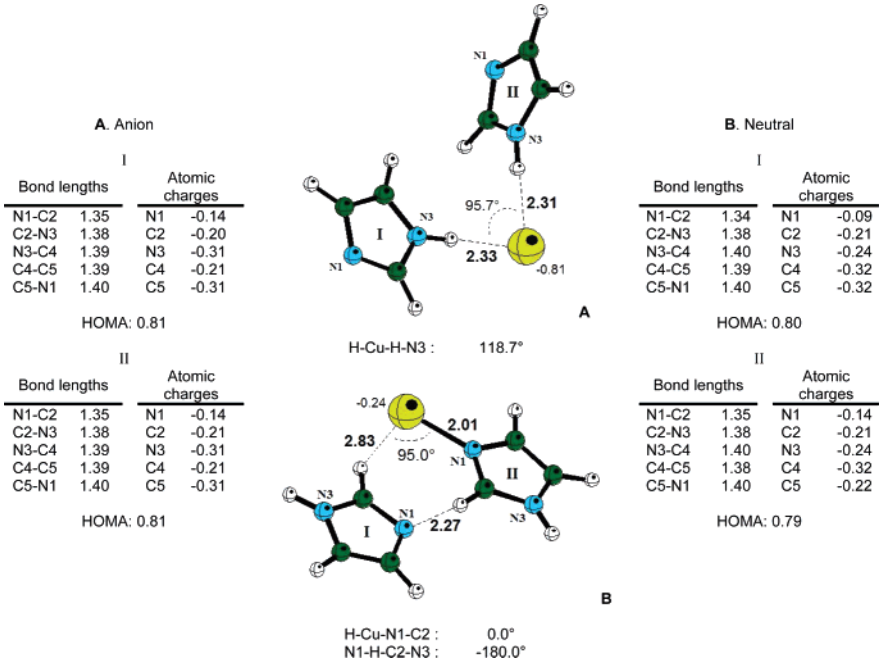

[a] Bond lengths are in Å, atomic charges in au.

Table 7. Anionic (**A**) and Neutral (**B**) $(C_3H_3N_2)_2Cu$ Optimized Geometries[a]

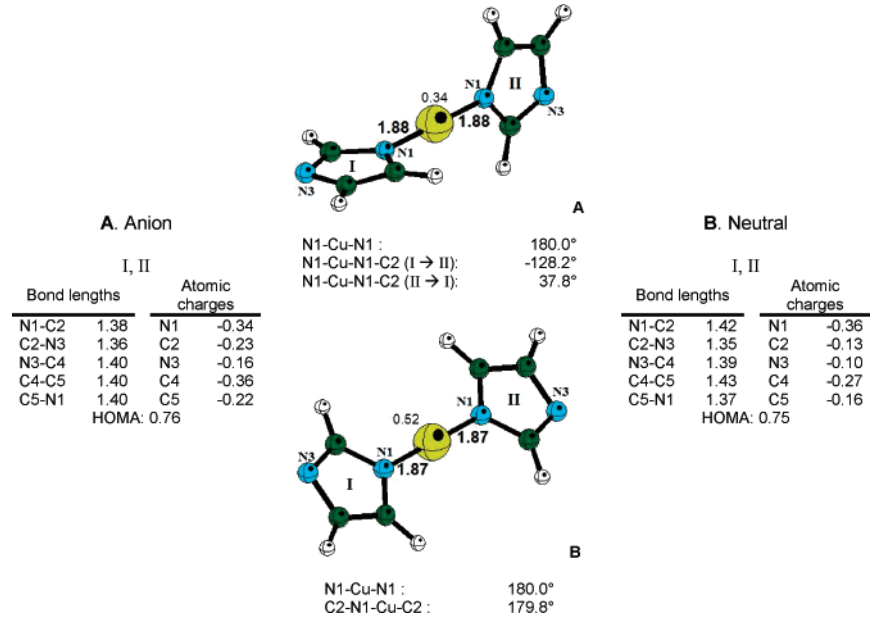

[a] Bond lengths are in Å, atomic charges in au.

methodology, since the MP2 calculations agree with the experimental results that they also reported.

After this validation, we can compare the bond distances shown in Table 3 for the neutral and the anionic species. The bond length is shorter for the neutral than for the anionic. The electron repulsion between the N lone-pairs and the Cu 4s electrons is higher in the anion, due to the fact that the extra electron is located on the metal atom. This corresponds with the values for the electron affinity, given that, for copper, it is higher than for the imidazole. The negative metal atom is moved from the nitrogen atom in the neutral to an hydrogen atom in the anion.

In order to analyze the effect of the dissociation of one hydrogen atom, in Table 4, the optimized structures for (Cu−imidazole)−H compounds ($C_3H_4N_2Cu$, neutral and anionic) are reported. As may be observed, when the hydrogen atom is removed, the Cu−N bond distance shortens in both systems, neutral and anionic. The electron repulsion is reduced because the metal atom is less negative (for the neutral it becomes positive), and the extra electron of the

Table 8. Anionic (**A**) and Neutral (**B**) $(C_3H_4N_2)_3Cu$ Optimized Geometries

A. Anion

I, II

Bond lengths		Atomic charges	
N1-C2	1.36	N1	-0.27
C2-N3	1.39	C2	-0.09
N3-C4	1.40	N3	-0.37
C4-C5	1.38	C4	-0.26
C5-N1	1.41	C5	-0.16

HOMA: 0.73

III

Bond lengths		Atomic charges	
N1-C2	1.47	N1	-0.27
C2-N3	1.47	C2	-0.30
N3-C4	1.38	N3	-0.27
C4-C5	1.42	C4	-0.39
C5-N1	1.38	C5	-0.39

HOMA: 0.22

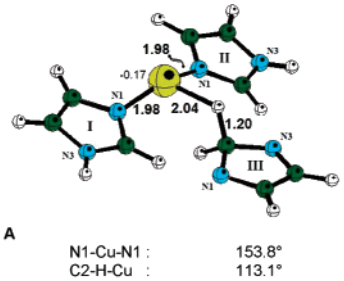

A

N1-Cu-N1 : 153.8°
C2-H-Cu : 113.1°

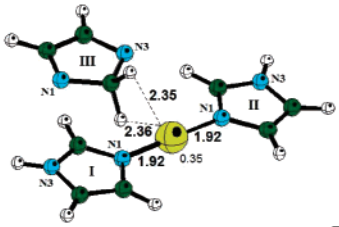

B

B. Neutral

I, II

Bond lengths		Atomic charges	
N1-C2	1.36	N1	-0.32
C2-N3	1.37	C2	-0.04
N3-C4	1.40	N3	-0.35
C4-C5	1.38	C4	-0.22
C5-N1	1.41	C5	-0.15

HOMA: 0.77

III

Bond lengths		Atomic charges	
N1-C2	1.49	N1	-0.24
C2-N3	1.49	C2	-0.31
N3-C4	1.37	N3	-0.24
C4-C5	1.43	C4	-0.34
C5-N1	1.37	C5	-0.34

HOMA: 0.02

[a] Bond lengths are in Å, atomic charges in au.

Table 9. Anionic (**A**) and Neutral (**B**) $(C_3H_4N_2)_2Cu(C_3H_2N_2)$ Optimized Geometries

A. Anion

I, II

Bond lengths		Atomic charges	
N1-C2	1.35	N1	-0.22
C2-N3	1.38	C2	-0.03
N3-C4	1.40	N3	-0.37
C4-C5	1.39	C4	-0.26
C5-N1	1.40	C5	-0.24

HOMA: 0.79

III

Bond lengths		Atomic charges	
N1-C2	1.40	N1	-0.39
C2-N3	1.40	C2	0.04
N3-C4	1.40	N3	-0.45
C4-C5	1.41	C4	-0.37
C5-N1	1.40	C5	-0.38

HOMA: 0.67

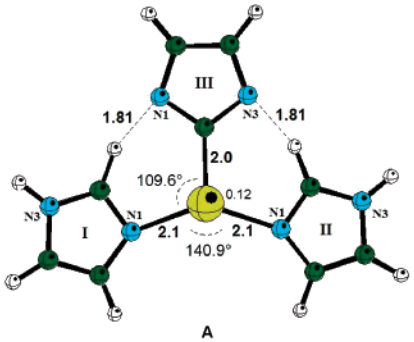

A

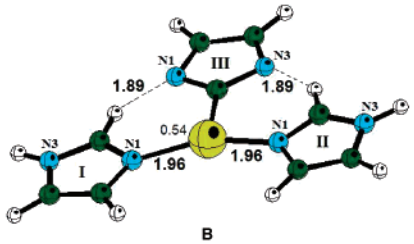

B

N1-Cu-N1 : 151.0°
N1-Cu-C2 (I→III): 104.5°

B. Neutral

I, II

Bond lengths		Atomic charges	
N1-C2	1.35	N1	-0.32
C2-N3	1.37	C2	-0.02
N3-C4	1.40	N3	-0.35
C4-C5	1.38	C4	-0.22
C5-N1	1.40	C5	-0.16

HOMA: 0.80

III

Bond lengths		Atomic charges	
N1-C2	1.36	N1	-0.26
C2-N3	1.36	C2	0.08
N3-C4	1.40	N3	-0.26
C4-C5	1.41	C4	-0.35
C5-N1	1.40	C5	-0.35

HOMA: 0.81

[a] Bond lengths are in Å, atomic charges in au.

anion is spread over the imidazole molecule. Therefore, the negative charge is mainly located on the carbon atoms instead of on the nitrogen atoms. Concerning the aromaticity, as the HOMA values indicate in Tables 3 and 4, the imidazole molecule is more aromatic in the anionic than in the neutral. The extra electron is responsible for this behavior.

With these structures we can analyze the reaction for the production of molecular hydrogen, as can be seen in Table 5. Considering the neutral systems, the dehydrogenation reaction to produce H_2 is energetically unfavorable. However, the formation of H_2 from Cu−imidazole anion is favorable (−12.8 kcal/mol).

The results for the species with one copper atom and two imidazole molecules are quite similar, as can be seen in Tables 6 and 7. For the neutrals, the structures with and without two hydrogen atoms are planar, while, for the anions, the imidazole molecules are not in the same plane. Cu−N bond lengths are almost the same for the neutral and the anion Cu−(imidazole)$_2$−2H systems ($(C_3H_3N_2)_2Cu$), see Table 7), and these bonds are shorter than the same bonds of the Cu−(imidazole)$_2$ species. The atomic charge of the copper atom is negative for complexes with full imidazole molecules, as can be seen in Table 6, where the negative metal atom is oriented toward the positive hydrogen atoms. Conversely, copper atoms are positive on the Cu−(imidazole)$_2$−2H complexes. From this, we can infer that the positive metal atomic charge promotes the bond with the nitrogen atom (negatively charged). The aromaticity of

imidazole molecules on these species is more or less the same. The less aromatic compound is Cu−(imidazole)$_2$−2H neutral. Departing from these structures, we analyzed the dehydrogenation reaction in order to obtain H_2. The results are reported in Table 5. It may be observed that the reaction for the anionic system is energetically favorable (−48.9 kcal/mol), whereas for the neutral, the products of the reaction are less stable than the reactants, by 7 kcal/mol.

In Tables 8 and 9, the most stable optimized structures of Cu−(imidazole)$_3$ and Cu−(imidazole)$_3$−2H ($(C_3H_3N_2)_2$Cu-$(C_3H_2N_2)$, neutral and anionic) are reported. As can be seen, the results are similar to those for the optimized structures with one and two imidazole molecules. The most stable structures of Cu−(imidazole)$_3$ (neutral and anionic) contain one isomer of the imidazole having two hydrogen atoms bonded to one carbon atom and nitrogen atoms that have no hydrogens. The interaction of copper and two imidazole molecules takes place on two negatively charged nitrogen atoms and, moreover, forms a "bridge" with two hydrogen atoms of the opposite imidazole molecule. When two hydrogen atoms are detached, the structures are planar and two N−H interactions are formed. The metal atom is connected to the three molecules, from one carbon atom and two nitrogen atoms. HOMA values indicate that the imidazole molecule that contains two hydrogen atoms bonded to a carbon atom is less aromatic, as could be anticipated from the bond distances. When one hydrogen atom is detached, in the neutral molecule, the HOMA values indicate that the aromaticity of the imidazole molecules is the same, while for the anionic it is different. One imidazole molecule situated in the middle is less aromatic than the others. In Table 5, it may be observed that the dehydrogenation reaction is energetically stable for the anion, but not for the neutral, as was found for the species with one and two imidazole molecules.

Comparing the formation energies for the three systems under study, we may say that the most favorable reaction is the one where the copper atom is more positive (+0.33 in Cu−(imidazole)$_2$−2H). The formation energy is proportional to the positive charge of the copper atom on the dehydrogenated products. It appears that there is a charge-transfer process from the copper atom to the nitrogen atoms of the imidazole molecules. When this charge transfer is large, the interaction energy is similarly large. For the thermodynamically stable production of H_2 from Cu−(imidazole)$_N$, the species must be anionic.

Conclusions

Two systems were considered for the study of metal−molecule interactions that can lead to the production of molecular hydrogen: yttrium atom and clusters interacting with the simple electron donor ammonia (NH_3) and copper atoms and ions with imidazole.

For yttrium with ammonia, oxidative addition is the first step of the reaction where the imide species is formed; however, yttrium atoms could also interact, forming yttrium dimers as a result. If ammonia is the limiting reactant, it is most probable that YNH will react with Y, Y_2NH, and Y_2N. If Y_2 is already formed, the addition of one ammonia molecule to Y_2 to form $Y_2NH + H_2$ will occur. If the dimer is not formed, because ammonia is in excess and the most probable reaction then is the formation of YNH, we may consider that the sequential addition of three further NH_3 molecules to YNH, in order to produce the diamide species, is a possible reaction. To avoid competition with the diamide formation, it is preferable to have ammonia as the limiting reactant. From this analysis, it is possible to conclude that the optimum reactions for the production of H_2 are those with Y_2NH and YNH and Y_2 with ammonia.

For copper with imidazole, the dehydrogenation reaction is energetically stable for the anion but not for the neutral. For yttrium with ammonia as well as for copper with imidazole there is a charge-transfer process from the metal to the molecule that promotes the dissociation of the hydrogen atoms. Further studies are required if conclusions are to be drawn regarding the common characteristics necessary in the metal−molecule interactions, in order to produce molecular hydrogen. It is important that we learn more about the energetic barriers, the interaction of copper with ammonia, and also the interaction of yttrium with imidazole, in order to be able to make a complete comparison between these two systems. Calculations are in progress with a view to answering these questions and also in understanding the relationship between the reactivity and the size of the metal clusters.

Acknowledgment. This study was made possible due to funding supplied by DGAPA-PAPIIT, grant no. IN124602-3, and the Consejo Nacional de Ciencia y Tecnología (CONACyT) of Mexico, grant no. 69878, and the resources made available to us by the Instituto de Investigaciones en Materiales (IIM). Conversations with Benoit Simard from the Steacie Institute of Ottawa, Canada were invaluable in clarifying many aspects of this work. The authors would like to acknowledge Sara Jiménez Cortés and María Teresa Vázquez for their technical support and DGSCA/UNAM (México) for providing computer time.

References

(1) Barbarossa, V.; Brutti, S.; Diamanti, M.; Sau, S.; De Maria, G. *Int. J. Hydrogen Energy* **2006**, *31*, 883−890.

(2) Sigurvinsson, J.; Mansilla, C.; Arnason, B.; Botemps, A.; Maréchal, A.; Sigfusson, T. I.; Werkoff, F. *Energy Convers. Manage.* **2006**, *47*, 3543−3551.

(3) Schilling, J. B.; Goddard, W. A., III; Beauchamp, J. L. *J. Am. Chem. Soc.* **1986**, *108*, 582−584.

(4) Schilling, J. B.; Goddard, W. A., III; Beauchamp, J. L. *J. Am. Chem. Soc.* **1987**, *109*, 5573−5580.

(5) Elkind, J. L.; Armentrout, P. B. *Inorg. Chem.* **1986**, *25*, 1078−1080. Armentrout, P. B.; Halle, L. F.; Beauchamp, J. L. *J. Chem. Phys.* **1982**, *76*, 2449−2457.

(6) Knight, L. B., Jr.; Cobranchi, S. T.; Herlong, J.; Kirk, T.; Balasubramanian, K.; Das, K. K. *J. Chem. Phys.* **1990**, *92*, 2721−2732.

(7) Geusic, M. E.; Morse, M. D.; Smalley, R. E. *J. Chem. Phys.* **1985**, *82*, 590−591.

(8) Morse, M. D.; Geusic, M. E.; Heath, J. R.; Smalley, R. E. *J. Chem. Phys.* **1985**, *83*, 2293−2304.

(9) Richtsmier, S. C.; Parks, E. K.; Liu, K.; Pobo, L. G.; Riley, R. E. *J. Chem. Phys.* **1985**, *82*, 3659−3665.

(10) Whetten, R. L., Zakin, M. R.; Cox, D. M.; Trevor, D. J.; Kaldor, A. *J. Chem. Phys.* **1986**, *85*, 1697−1698.

(11) Low, J. J.; Goddard, W. A., III *Organometallics* **1986**, *5*, 609−622.

(12) Bühl, M.; Kabrede, H. *J. Chem. Theory Comput.* **2006**, *2*, 1282−1290.

(13) Balasubramanian, K.; Liao, M. Z. *J. Phys. Chem.* **1989**, *93*, 89−94.

(14) Balasubramanian, K. *Int. J. Quantum Chem. Symp.* **1988**, *22*, 465−476.

(15) Backwall, J. E.; Bjorkman, E. E.; Petterson, L.; Siegbahn, P. E. M. *J. Am. Chem. Soc.* **1985**, *107*, 7265−7267.

(16) Das, K. K.; Balasubramanian, K. *J. Chem. Phys.* **1989**, *91*, 2433−2442.

(17) Das, K. K.; Balasubramanian, K. *J. Chem. Phys.* **1990**, *93*, 6671−6675.

(18) Zakin, M. R.; Cox, D. M.; Kaldor, A. *J. Phys. Chem.* **1987**, *91*, 5224−5228.

(19) Zakin, M. R.; Brickman, R. O.; Cox, D. M.; Kaldor, A. *J. Chem. Phys.* **1988**, *88*, 5943−5947.

(20) Berg, C.; Schindler, T.; Lammers, A.; Niedner-Schatteburg, G.; Bondybey, V. E. *J. Phys. Chem.* **1995**, *99*, 15497−15501.

(21) Parnis, J. M., Escobar-Cabrera, E.; Thompson, M. G. K.; Jacula, J. P.; Lafleur, R. D.; Guevara-Garcia, A.; Martínez, A.; Rayner, D. M. *J. Phys. Chem. A* **2005**, *109*, 7046−7056.

(22) Rivalta, I.; Russo, N.; Sicilia, E. *J. Mol. Struct. (THEOCHEM)* **2006**, *762*, 25−31.

(23) Martínez, A. *J. Chem. Phys.* **2005**, *123*, 024311(1−9).

(24) Spessard, G. O.; Miessler, G. L. *Organometallic Chemistry*; Prentice Hall: Upper Saddle River, NJ, 1996; pp 245−299.

(25) Simard, B.; Jakubec, Z. *J. Chem. Phys.* **1999**, *111*, 1483−1493.

(26) Kohn, W.; Becke, A. D.; Parr, R. G. *J. Phys. Chem.* **1996**, *100*, 12974−12980.

(27) Hohenberg, P.; Kohn, W. *Phys. Rev.* **1964**, *136*, B864−B871.

(28) Kohn, W.; Sham, L. J. *Phys. Rev.* **1965**, *140*, A1133−A1138.

(29) Frisch, M. J.; Trucks, G. W.; Schlegel, H. B.; Scuseria, G. E.; Robb, M. A.; Cheeseman, J. R.; Montgomery, J. J. A.; Vreven, T.; Kudin, K. N.; Burant, J. C.; Millam, J. M.; Iyengar, S. S.; Tomasi, J.; Barone, V.; Mennucci, B.; Cossi, M.; Scalmani, G.; Rega, N.; Petersson, G. A.; Nakatsuji, H.; Hada, M.; Ehara, M.; Toyota, K.; Fukuda, R.; Hasegawa, J.; Ishida, M.; Nakajima, T.; Honda, Y.; Kitao, O.; Nakai, H.; Klene, M.; Li, X.; Knox, J. E.; Hratchian, H. P.; Cross, J. B.; Bakken, V.; Adamo, C.; Jaramillo, J.; Gomperts, R.; Stratmann, R. E.; Yazyev, O.; Austin, A. J.; Cammi, R.; Pomelli, C.; Ochterski, J. W.; Ayala, P. Y.; Morokuma, K.; Voth, G. A.; Salvador, P.; Dannenberg, J. J.; Zakrzewski, V. G.; Dapprich, S.; Daniels, A. D.; Strain, M. C.; Farkas, O.; Malick, D. K.; Rabuck, A. D.; Raghavachari, K.; Foresman, J. B.; Ortiz, J. V.; Cui, Q.; Baboul, A. G.; Clifford, S.; Cioslowski, J.; Stefanov, B. B.; Liu, G.; Liashenko, A.; Piskorz, P.; Komaromi, I.; Martin, R. L.; Fox, D. J.; Keith, T.; Al-Laham, M. A.; Peng, C. Y.; Nanayakkara, A.; Challacombe, M.; Gill, P. M. W.; Johnson, B.; Chen, W.; Wong, M. W.; Gonzalez, C.; Pople, J. A. Gaussian, Inc.: Wallingford CT, 2004.

(30) Becke, A. D. *Phys. Rev. A* **1988**, *38*, 3098−3100.

(31) Mielich, B.; Savin, A.; Stoll, H.; Preuss, H. *Chem. Phys. Lett.* **1989**, *157*, 200−206.

(32) Lee, C.; Yang, W.; Parr, R. G. *Phys. Rev. B* **1988**, *37*, 785−789.

(33) Hay, P. J.; Wadt, W. R. *J. Chem. Phys.* **1985**, *82*, 270−283.

(34) Hay, P. J.; Wadt, W. R. *J. Chem. Phys.* **1985**, *82*, 299−310.

(35) Wadt, W. R. *J. Chem. Phys.* **1985**, *82*, 284−298.

(36) Foresman, J. B.; Frisch, Æ. *Exploring Chemistry with Electronic Structure Methods*, 2nd ed.; Gaussian, Inc.: Pittsburgh, PA, 1996; pp 61−90.

(37) Ochterski, J. W. *Vibrational analysis in Gaussian*; Gaussian, Inc.: Pittsburgh, PA, 1999; p 10.

(38) Shishkin, O. V.; Gorb, L.; Luzanov, A. V.; Elstner, M.; Suhai, S.; Leszczynski, J. *J. Mol. Struct. (THEOCHEM)* **2003**, *625*, 295−303.

(39) Møller, C.; Plesset, M. S. *Phys. Rev.* **1934**, *46*, 618−622.

(40) Saebo, S.; Almlof, J. *Chem. Phys. Lett.* **1989**, *154*, 83−89.

(41) de Oliveira, A. E.; Guadagnini, P. H.; Haiduke, R. L. A.; Bruns, R. E. *J. Phys. Chem. A* **1999**, *103*, 4918−4924.

(42) Kruszewski, J.; Krygowski, T. M. *Tetrahedron Lett.* **1972**, *13*, 3839−3842.

(43) Krygowski, T. M. *J. Chem. Inf. Comput. Sci.* **1993**, *33*, 70−78.

(44) Krygowski, T. M.; Anulewicz, R.; Kruszewski, J. *Acta Crystallogr., Sect. B: Struct. Sci.* **1983**, *B39*, 732−739.

(45) Krygowski, T. M.; Cyranski, M. K. *Tetrahedron* **1996**, *52*, 10255−10264.

(46) Krygowski, T. M.; Cyranski, M. K. *Chem. Rev.* **2001**, *101*, 1385−1420.

(47) Schaftenaar, G.; Noordik, J. H. *J. Comput.-Aided. Mol. Des.* **2000**, 14, 123−134 (Molden).

(48) Flükiger, P.; Lüthi, H. P.; Portmann, S.; Weber, J. 4.3 ed.; Swiss Center for Scientific Computing: Manno, Switzerland, 2000−2002.

(49) Portmann, S.; Lüthi, H. P. *Chimia* **2000**, *54*, 766−770.

(50) Müller, N.; Falk, A. 3.75 ed.; Johannes Kepler University: Linz, 2000.

(51) Simard, B., private communication.

(52) (a) Simard, B.; Rayner, D. M.; Benichou, E.; Mireles, N.; Tenorio, F. J.; Martínez A. *J. Phys. Chem. A* **2003**, *107*, 9099−9104. (b) Martínez, A. *J. Phys. Chem. A* **2006**, *110*, 1978−1981.

(53) Sundberg, R. J.; Martin, R. B. *Chem. Rev.* **1974**, *74*, 471−517.

(54) Wang, X.; Sup-Lee, J.; Yang, D. S. *J. Phys. Chem. A* **2006**, *110*, 12777−12784.

CT6003615